



Published in final edited form as:

Fertil Steril. 2019 April ; 111(4): 794–805. doi:10.1016/j.fertnstert.2018.12.015.

Extracellular matrix signaling activates differentiation of adult ovary-derived oogonial stem cells in a species-specific manner

Julie A. MacDonald, B.S.^a, Yasushi Takai, M.D., Ph.D.^b, Osamu Ishihara, M.D., Ph.D.^b, Hiroyuki Seki, M.D., Ph.D.^b, Dori C. Woods, Ph.D.^a, and Jonathan L. Tilly, Ph.D.^a

^aLaboratory of Aging and Infertility Research, Department of Biology, Northeastern University, Boston, Massachusetts

^bDepartment of Obstetrics and Gynecology, Saitama Medical Center, Saitama Medical University, Saitama, Japan

Abstract

Objective: To test if ovarian microenvironmental cues affect oogonial stem cell (OSC) function in a species-specific manner.

Design: Animal and human study.

Setting: Research laboratory.

Patient(s)/Animal(s): Human ovarian cells obtained from cryopreserved ovarian cortical tissue of reproductive-age women, and ovarian cells and tissues from female C57BL/6 mice.

Intervention(s): Mouse ovarian tissue, mouse OSCs (mOSCs) and human OSCs (hOSCs) were analyzed for extracellular matrix (ECM) protein expression, and OSCs isolated from adult mouse and human ovaries were cultured in the absence or presence of ECM proteins without or with an integrin signaling inhibitor.

Main Outcome Measure(s): Gene expression and in vitro derived (IVD) oocyte formation.

Result(s): Culture of mOSCs on a collagen-based ECM significantly elevated the rate of differentiation of the cells into IVD oocytes. Mouse OSCs expressed many integrins, including Arg-Gly-Asp (RGD)-binding subunits, and ECM-mediated increases in mOSC differentiation were blocked by addition of integrin-antagonizing RGD peptides. In comparison, hOSCs expressed a different pattern of integrin subunits compared with mOSCs, and hOSCs were unresponsive to a collagen-based ECM; however, hOSCs exhibited increased differentiation into IVD oocytes when cultured on laminin.

Reprint requests: Jonathan L. Tilly, Ph.D., Department of Biology, 134 Mugar Life Sciences Building, Northeastern University, 360 Huntington Avenue, Boston, Massachusetts 02115 (j.tilly@northeastern.edu).

J.A.M. has nothing to disclose. Y.T. has nothing to disclose. O.I. has nothing to disclose. H.S. has nothing to disclose. D.C.W. discloses interest in intellectual property described in U.S. Patent 8,642,329, U.S. Patent 8,647,869 and U.S. Patent 9,150,830. J.L.T. discloses interest in intellectual property described in U.S. Patent 7,195,775, U.S. Patent 7,850,984, U.S. Patent 7,955,846, U.S. Patent 8,642,329, U.S. Patent 8,647,869, U.S. Patent 8,652,840, U.S. Patent 9,150,830, U.S. Patent 9,267,111 and U.S. Patent 9,845,482 and is a scientific cofounder of Ovascience.

Conclusion(s): These data, along with in silico analysis of ECM protein profiles in human ovaries, indicate that ovarian ECM-based niche components function in a species-specific manner to control OSC differentiation.

Keywords

Germline stem cell; oogenesis; oocyte; ovary; matrix

For many years, it was widely thought that ovarian failure with age in mammals resulted from progressive loss and ultimately exhaustion of a nonrenewable pool of oocyte-containing follicles endowed in the ovaries at birth (1–4). However, the identification of female germline or oogonial stem cells (OSCs) in postnatal mouse ovaries in 2004 (5) raised significant questions about the validity of this longstanding paradigm. Although initially met with skepticism (6, 7), subsequent studies characterizing oogenesis and OSCs in adult ovarian tissue of mice (8–35), rats (36), pigs (37, 38), cows (39), monkeys (40), and humans (14, 41–44) by many laboratories have offered new insights into possible causes and potential management of ovarian dysfunction and infertility beyond those posed by many of the traditional models used to describe mammalian ovarian development, function, and failure (45–50). For example, human OSCs have recently been tested in clinical studies as a source of autologous germline mitochondria for boosting egg and embryo quality in women with a history of repeated in vitro fertilization (IVF) failure (51–53). In addition, several studies have shown that OSCs persist in ovaries past the time of age-related failure in mice (8, 27) and humans (43, 53). While no longer supportive of active oogenesis in vivo (27), OSCs in aged ovaries apparently remain capable of generating oocytes if cultured under defined conditions ex vivo (43, 53) or if reexposed to a young ovarian environment in vivo (8). It should be emphasized, however, that whereas OSCs in mice and rats have been repeatedly shown to differentiate in vivo into functional eggs that produce viable embryos and offspring (9, 10, 14, 22, 25, 27, 28, 36), all studies of human OSCs to date have been limited to in vitro analyses (14, 41–44). Nonetheless, the findings discussed above (8, 27, 43, 53) indicate that a progressive decline in OSC function with age, as recently highlighted through a genetic model of inducible suicide gene-based cellular ablation in mice (27), may be due more to a loss of as yet unidentified external cues needed for OSC differentiation rather than intrinsic differentiation defects within OSCs.

The extracellular matrix (ECM) is a key regulator of embryonic (54–57) and adult (58) stem cell fate. In turn, aging-associated dysfunction of many organ systems is thought to arise, at least in part, from deterioration of a homeostatic relationship between resident regenerative stem cell populations and their supporting microenvironments (59–64). Although it is unknown if this stem cell–niche interaction model of tissue aging applies to ovaries, the adult female gonads have served as an insightful model for mechanistic studies of ECM function owing to the tremendous degree of repeated tissue remodeling associated with volumetric expansion of growing follicles, ovulatory rupture of the ovarian surface epithelium, and development of corpora lutea after ovulation that occurs in each reproductive cycle (65–67). In addition, interaction of activin-A with the ECM has been identified as a principal mechanism underlying the initiation of follicular growth in the mouse ovary (68). Herein we designed a series of experiments to expand existing knowledge

of the importance of ECM in adult ovarian function by assessing the potential role of ECM as a microenvironmental niche factor for the regulation of OSC differentiation in adult mouse and human ovaries.

MATERIALS AND METHODS

Reagents

All reagents were obtained from Thermo Fisher Scientific, unless otherwise indicated.

Animals

Wild-type C57BL/6 mice (6 weeks of age) were obtained from Charles River Laboratories, and aged for each experiment. All experimental procedures reported herein were reviewed and approved by the Institutional Animal Care and Use Committee of Northeastern University.

Human Ovarian Tissues

Adult ovarian cortical tissue was collected from three reproductive-age women (22, 24, and 33 years of age) undergoing sex reassignment at Saitama Medical Center and then cryopreserved via vitrification until use (14). As described subsequently, OSC lines were independently established from each of the three ovarian cortical tissue samples for experimental study. All procedures with human ovarian tissue and cells were reviewed and approved by the Institutional Review Boards at Northeastern University and Saitama Medical University.

Histology and Immunohistochemistry

Ovaries collected from mice at 2, 12, and 20 months of age (three animals per age group for independent analysis) were fixed and processed for paraffin embedding and serial section analysis (5–15 6-mm sections analyzed per ovary, with both ovaries from each of the three mice per age group assessed in parallel). Some sections were stained with the use of Weigert iron hematoxylin and a picric acid methyl blue counterstain. Other sections were stained with the use of a variation of van Gieson stain, composed of celestin blue (Sigma-Aldrich), Weigert iron hematoxylin, and Curtis substitute of saturated picric acid with ponceau S (Sigma-Aldrich) and glacial acetic acid, to differentiate collagen (red), nuclei (blue), and cytoplasm (yellow). Colorimetric photomicrographs were obtained with the use of a Zeiss Axioplan microscope and analyzed for gross tissue morphology, collagen organization, and histologic evidence of fibrosis or stromal hyperplasia (69). Additional sections of ovaries from the same animals were processed for indirect immunolabeling of type I collagen (with the use of an antibody against the collagen Ia1 subunit; Novus Biologicals NB600–408) and type IV collagen (with the use of an antibody against the collagen IV α 1 subunit; Novus Biologicals NB120–6586) using temperature-based antigen retrieval in citrate buffer (10 mmol/L, pH 6.0). After washing, the sections were incubated in a blocking buffer containing 1% normal goat serum, 2% bovine serum albumin, and 0.1% Triton-X in phosphate-buffered saline solution (PBS), washed, and incubated in 10- μ g/mL solutions of each primary antibody overnight at 4°C overnight. After washing in PBS, the sections were incubated in a 1- μ g/mL solution of a Dylight 650 secondary antibody (Invitrogen) for 1 hour in the dark at

room temperature. Sections were then washed of excess antibody in PBS and counterstained with a 1- $\mu\text{g}/\text{mL}$ solution of Hoechst 33342 before mounting in Prolong Gold mounting medium. After all slides had cured, images were obtained with the use of a Zeiss Axioplan microscope, with fluorescence exposure time optimized in each channel with the use of ovarian tissue of 12-month-old mice and maintained throughout imaging, including slides which received no primary antibody as negative control samples. Although the ovarian ECM consists of more than these two types of collagen, we chose to focus on these proteins because they are well characterized ECM constituents in both mouse (67, 70) and human (71) ovaries and are often used in the field of regenerative biology for the manufacture of biomimetic tissues (72).

Hydroxyproline Assay

Levels of hydroxyproline, which is found nearly exclusively in collagen and is widely used as a measure of changes in collagen content (73), were assayed in ovaries of mice at 2, 12, and 20 months of age ($n = 5\text{--}6$ mice per age group) with the use of a commercially available kit (Cell Biolabs) following the manufacturer's protocol.

Oogonial Stem Cell Isolation, Culture, and In Vitro Differentiation

As detailed previously (14, 17), OSCs were isolated from pooled ovaries of four 2-month-old mice or from human ovarian cortical tissue by means of fluorescence-activated cell sorting via immunolabeling of the dispersed tissue with the use of a polyclonal antibody directed against the C-terminus of DDX4 (Abcam). Purified OSCs were maintained in culture as previously described (14, 17) and used for all experiments in passages 30–35 for mouse OSCs (mOSCs), and passages 15–20 for human OSCs (hOSCs). To monitor differentiation, 2.5×10^4 OSCs were plated in triplicate wells in plastic 24-well tissue culture plates containing 0.5 mL OSC culture medium for each experimental replicate. At 24-hour intervals, 20% of the culture medium (0.1 mL) was sampled and evaluated by means of light microscopy for the number of in vitro derived (IVD) oocytes (14, 16, 17, 35, 41, 43). After IVD oocytes in each well had been counted, the spent medium was removed and replaced with 0.5 mL fresh culture medium to evaluate IVD oocyte generation over the next time interval. This approach was taken based on prior experiments showing that purified OSCs maintained as pure germ cell cultures can spontaneously differentiate into IVD oocytes (14, 43) through a differentiation process dependent on the key driver of in vivo meiotic commitment, *Stra8* (27). In addition to serving as a reliable bioassay to more definitively explore the oogenic activity of factors already known to influence early germ cell development (e.g., bone morphogenetic protein 4) (16), measurement of IVD oocyte generation in OSC cultures can also accurately predict the in vivo effects of as yet untested experimental manipulations on endogenous oocyte formation (27). To study the impact of ECM proteins on OSC differentiation, tissue culture plates were thinly coated ($10 \mu\text{g}/\text{cm}^2$) with laminin (Novus Biologicals), type I collagen (Cultrex), type IV collagen (Cultrex), or an equal mixture of type I and type IV collagens, according to the manufacturer's instructions for each protein, before cell plating. In some experiments, receptor-neutralizing doses ($500 \mu\text{mol}/\text{L}$) of Arg-Gly-Asp (RGD) peptides (Abcam) were used to inhibit binding of integrins to ECM proteins.

Gene Expression Analysis

Cultures were prepared as described above, and total RNA was extracted with the use of an RNeasy Micro kit (Qiagen). Isolated RNA was then normalized in concentration across samples to be analyzed and treated with the use of DNase-I to remove potential genomic DNA contamination, followed by first-strand cDNA synthesis with the use of a Revertaid reverse-transcription kit. Quantitative analysis of *stimulated by retinoic acid gene 8 (Stra8)* expression was performed with the use of a Taqman gene expression assay against *Stra8* (assay ID Mm00486473_m1) and a housekeeping reference gene (*glyceraldehyde 3-phosphate dehydrogenase [GAPDH]*; assay ID Mm99999915_g1). Integrin expression profiles for mOSCs were determined by means of conventional reverse-transcription (RT) polymerase chain reaction (PCR) with the use of Gotaq Green (Promega) and primers described in Supplemental Table 1 (available online at www.fertstert.org). Integrin expression profiles for hOSCs were determined with the use of Fast Sybr Green (Life Technologies) and primers for real-time PCR included in the Human Integrin Signaling Primer Library (realtimeprimers.com) and use of the Steponeplus Real-Time PCR System (Applied Biosystems). Relative levels of gene expression were classified as “high (+++)” if the target gene was detected before detection of *GAPDH*, “moderate (++)” if the target gene was detected within five cycles of detection of *GAPDH*, and “low (+)” if the target gene was detected more than five cycles after detection of *GAPDH*. Data presented include only those genes detected in all three hOSC lines, with each line established from a different subject. The complete data set is available in Supplemental Table 2 (available online at www.fertstert.org).

In Silico Proteomic Analysis

Quantitative mass spectrometry proteomics data analyzed in this study were retrieved from the Proteomexchange consortium (proteomecentral.proteomexchange.org) using PXD006898 as the identifier of the data set (44). This public data repository contains results from quantitative mass spectrometric analysis of fetal human ovarian tissue at gestational days 47, 108, 122, and 137 and of adult human ovarian cortex (44). All data were filtered to exclude any identified proteins not previously annotated as components of the “matrisome” (74, 75) and further filtered to include only those proteins identified in all samples, allowing for quantitative comparison based on the intensity-based absolute quantification method (44).

Data Presentation and Analysis

All experiments were independently replicated at least three times with the use of different mice or tissues and cells collected from different mice or human subjects, for each biologic replicate. Quantitative results are presented as the mean \pm SEM of the combined results across all replicate experiments, with statistical significance determined by means of analysis of variance with the post hoc Tukey Honestly Significant Difference (HSD) test. Qualitative data (histology, immunofluorescence, RT-PCR) are representative of results obtained in at least three independent biological replicates for each experiment.

RESULTS

Aging Mouse Ovarian Tissue Exhibits Evidence of Fibrotic Scarring and Dysregulated ECM Expression

Gross morphologic evaluation of mouse ovaries with increasing age (young adult, 2 months; midlife adult with pending reproductive compromise, 12 months; aged adult, 20 months) highlighted dramatic changes in overall tissue *organization* (Figs. 1A–1D). Collagenous bundles, exemplified most clearly by distinct basement membranes surrounding follicles in ovaries of young adult mice (Fig. 1A), became increasingly disorganized with age (Figs. 1B–1D). Most notably, collagen deposition became more global throughout the ovarian stroma, contrasting the discrete and tightly regulated localization of collagen detected in young adult ovaries. By 20 months, the tissue exhibited a broad and heterogeneous distribution of collagen throughout (Figs. 1C and 1D), including patches of fibrosis or stromal hyperplasia (69) as indicated by the strong, sporadic, red-stained regions within the vascularized medullary region of the ovaries (Fig. 1D).

To support and extend these qualitative assessments, ovaries were assayed for levels of the collagen-selective amino acid, hydroxyproline. Using ovaries of 2-month-old mice ($n = 6$) as a comparative baseline, hydroxyproline levels were elevated, but not significantly, by 12 months of age (mean \pm SEM 3.6 ± 1.3 -fold vs. 2 months of age; $n = 5$; $P = .19$); however, ovaries of mice at 20 months of age contained significantly higher levels of hydroxyproline (4.8 ± 1.3 -fold vs. 2 months of age; $n = 5$; $P < .05$), which is consistent with the aging-associated changes observed based on analysis of tissue morphology (Figs. 1A–1D).

We then performed immunolabeling of the main structural protein of the mouse ovary, type I collagen, and a major component of the follicular basement membrane, type IV collagen. Increased levels of type I collagen were detected throughout the ovaries with advancing age, along with the development of disorganized patches of fibrotic bundles in the stroma (Fig. 1E). In comparison, in young adult mouse ovaries type IV collagen was localized primarily within follicular basement membranes, with some expression evident in the stroma; however, by 20 months of age, ovarian expression of type IV collagen was minimal and confined primarily to the surface epithelial basement membrane (Fig. 1F).

Integrin-Mediated Signaling from Collagen Increases mOSC Differentiation

We next used the formation of IVD oocytes by cultured OSCs (Fig. 2A) as a model for the study of oogenesis to test if ECM proteins could functionally affect the differentiation capacity of these cells. Culture of mOSCs on an equal mixture of type I and type IV collagens for 72 hours increased IVD oocyte formation by 2.1 \pm 0.5-fold over those values in control cultures of OSCs maintained on uncoated tissue culture plastic (TCP; $n = 5$ independent cultures; $P < .05$ vs. TCP control samples; Fig. 2B). No significant differences in IVD oocyte formation occurred in cultures of OSCs maintained on type I collagen alone, type IV collagen alone, or laminin (Fig. 2B). Comparative gene expression analysis of freshly isolated and routinely passaged (cultured) mOSCs showed similar profiles of numerous integrin subunits with known matrix interaction capability (Figs. 2C and 2D), including the *Itga3*, *ItgaV*, *Itgb1*, and *Itgb3* RGD-binding subunits. Cultured mOSCs also

expressed *Itga10* and *Itga11*, which were not detected in freshly isolated cells (Figs. 2C and 2D). When OSCs were cultured on an equal mixture of type I and type IV collagens in the presence of a receptor-neutralizing concentration of RGD peptides, the enhanced level of oogenesis promoted by the collagen mixture was abolished (Fig. 2D). Likewise, expression of *Stra8* was increased 2.0 ± 0.6 -fold in OSCs cultured on a mixture of type I and type IV collagens ($n = 5$ independent cultures; $P < .05$ vs. TCP control samples), and this response was similarly abolished by RGD blockade (Fig. 2E).

Species-Specific Differences in ECM Sensitivity: Comparison of mOSCs and hOSCs

In contrast to the outcomes observed with the use of mOSCs, the number of IVD oocytes formed in cultures of hOSCs remained unchanged in the presence of not just type I collagen or type IV collagen but also an equal mixture of the two collagens; however, hOSCs cultured on laminin exhibited a significant increase in IVD oocyte formation at 48 and 72 hours of culture (3.2 ± 0.2 -fold and 2.2 ± 0.1 -fold increases, respectively, vs. TCP control samples; $n = 3$ independent cultures; $P < .01$; Figs. 3A–3D). Expression profiling analysis of hOSCs isolated from the three subjects indicated the presence of a diverse array of integrin signaling-related genes, grouped as integrin subunits, matrix deposition, matrix remodeling, and cell adhesion (Fig. 3E). Notably, hOSCs were found to express laminin, which promotes hOSC differentiation (Figs. 3A–3D). In addition, integrin subunit expression was far more limited in hOSCs (Fig. 3E) compared with mOSCs (Fig. 2B). We also observed that several gene products were not uniformly expressed across all three hOSC lines (Fig. 3E), indicative of both species-specific as well as individual-specific gene expression profiles.

In Silico Analysis of “Matrisome” Proteins in Human Ovaries

The striking differences detected in our comparative analyses of mOSCs versus hOSCs prompted us to further explore ECM profiles in human ovarian tissue through in silico analysis of matrix-related (“matrisome”) proteins, including core matrix components (glycoproteins, collagens, and proteoglycans) and matrix-associated components (ECM-affiliated proteins, ECM regulators, and secreted factors), with the use of a public data repository. Of the proteins identified with detectable levels of quantification in all five developmentally staged sample groups (Fig. 4A), two proteins exhibited the highest levels of expression in adult versus fetal ovaries at any stage: decorin (DCN) and lumican (LUM; Figs. 4B and 4C). At gestational day 122, we identified the highest relative expression of osteoglycin (OGN) and laminin gamma chain (LAMC1; Figs. 4D and 4E). At the earliest developmental stage analyzed, fibulin-1 (FBLN1) and protein C inhibitor (PCI) exhibited the highest levels of expression (Figs. 4F and 4G).

DISCUSSION

Although changes in the tissue microenvironment with age have been postulated to affect ovarian function and failure (8, 76), the present work has drawn the first functional links between known ovarian microenvironmental proteins and OSC differentiation capacity across species. Specifically, contact of mOSCs with both type I and type IV collagens activates higher levels of meiotic differentiation (*Stra8* expression) and oogenesis (IVD oocyte formation) through a pathway that involves interaction of the collagens with RGD

motif-binding integrin subunits. Because the expression profile of integrin subunits, including *Itga3*, *ItgaV*, *Itgb1*, and *Itgb3*, were similar in freshly isolated and cultured mOSCs, it is likely that these in vitro modeling data offer an accurate representation of the influence of ECM proteins on mOSC function in vivo. In contrast, we observed that hOSCs were unresponsive to collagen interaction but produced significantly more IVD oocytes when cultured on laminin. Interestingly, hOSCs were also found to express laminin, suggesting that these cells may produce their own ECM for long-term growth and differentiation. This finding may also explain the low basal rate of IVD oocyte formation detected in control hOSC cultures maintained on TCP.

In addition to identification of key targets for future studies of how changes in ECM may contribute to the loss of oogenic potential and ovarian aging (27), our results may help to inform the design of future bioengineering-based technologies for successful ex vivo reconstruction of human ovarian tissue which could be employed for many purposes, including potential new assisted reproductive therapies (46, 48, 50, 77). Most current systems being developed for in vitro egg production rely on use of existing primordial or primary follicles as input (72, 78, 79). These approaches fall short of serving as a truly regenerative biomimetic platform that incorporates proliferative female germ cells (e.g., OSCs) capable of expansion, meiotic entry, de novo oogenesis, and subsequent folliculogenesis (9, 14, 28, 36, 41, 42); however, achieving this goal would require that the germ cells are maintained in an appropriate microenvironment designed to maximize differentiation and growth. Detailed assessments of the ECM composition of the human ovary, as well as the ability to model adult oogenesis in vitro with the use of cultured OSCs under defined experimental conditions, has enabled a more robust identification and analysis of potential key components of this microenvironment, such as laminin. Results from the present study also indicate that a clear divergence exists in the differentiation potential of mouse versus human germ cells exposed to different ECM components, further highlighting the value of cultured OSCs as a rapid bioassay for identification of factors that drive female germ cell meiotic commitment and oogenesis in a species-specific manner (48).

Coupled with these comparative functional and gene expression studies of OSCs ex vivo, we also used in silico analysis of a public proteomics database to further delve into the identity of matrix factors that may be critical to the differentiation of human germ cells. This approach was taken to leverage the power of existing public databases in lieu of having liberal access to human ovarian cortical tissues collected throughout adult life and cryopreserved for detailed comparative analyses. To this end, a recent submission into the Proteomexchange consortium (44) studied, among other samples, fetal human ovaries at gestational day 47, when >90% of the germ cells present are premeiotic (undifferentiated) oogonia, versus gestational day 137, when more than three-fourths of the oogonia have differentiated into oocytes (80, 81). Many of the proteins we identified through in silico analysis of this database with detectable levels of quantification in all sample groups have rarely, if at all, been reported as matrix components in human ovaries outside of malignant ovarian tumor microenvironments. The latter include two proteins that exhibited the highest levels of expression in adult ovarian cortex versus developing fetal ovaries (at any stage): DCN and LUM. These proteins are small leucine-rich proteoglycans known to be associated with collagens in other tissues (82); however, both have only very recently been identified in

healthy human ovarian tissue (83) beyond a report of DCN in ovarian follicular fluid (84). At gestational day 122, a point in human ovarian development when oogonia are actively differentiating into oocytes, we identified the highest relative expression of OGN (also referred to as mimecan) and LAMC1. These findings add further support to the conclusion from our studies of hOSCs in vitro that, in human ovaries, laminin functions within a microenvironment that is supportive of oogenesis. Of additional interest, at the earliest developmental stage analyzed (gestational day 47), FBLN1 and PCI (also referred to as SERPINA5) had the highest levels of expression. Because FBLN1 has been linked to laminin binding (85), the increase in this protein just before the initial wave of human oogenesis during fetal life may reflect a role for this protein in laminin presentation to premeiotic germ cells as a mechanism to support meiotic differentiation. In addition, the identification of PCI in very-early-stage fetal human ovaries is consistent with a proposed role for this matrisome protein in sex differentiation (86).

Supplementary Material

Refer to Web version on PubMed Central for supplementary material.

Acknowledgments:

The authors thank Christina Yung for technical assistance.

Supported by a grant from the National Institutes of Health (NIH R01-AG012279 to J.L.T.).

REFERENCES

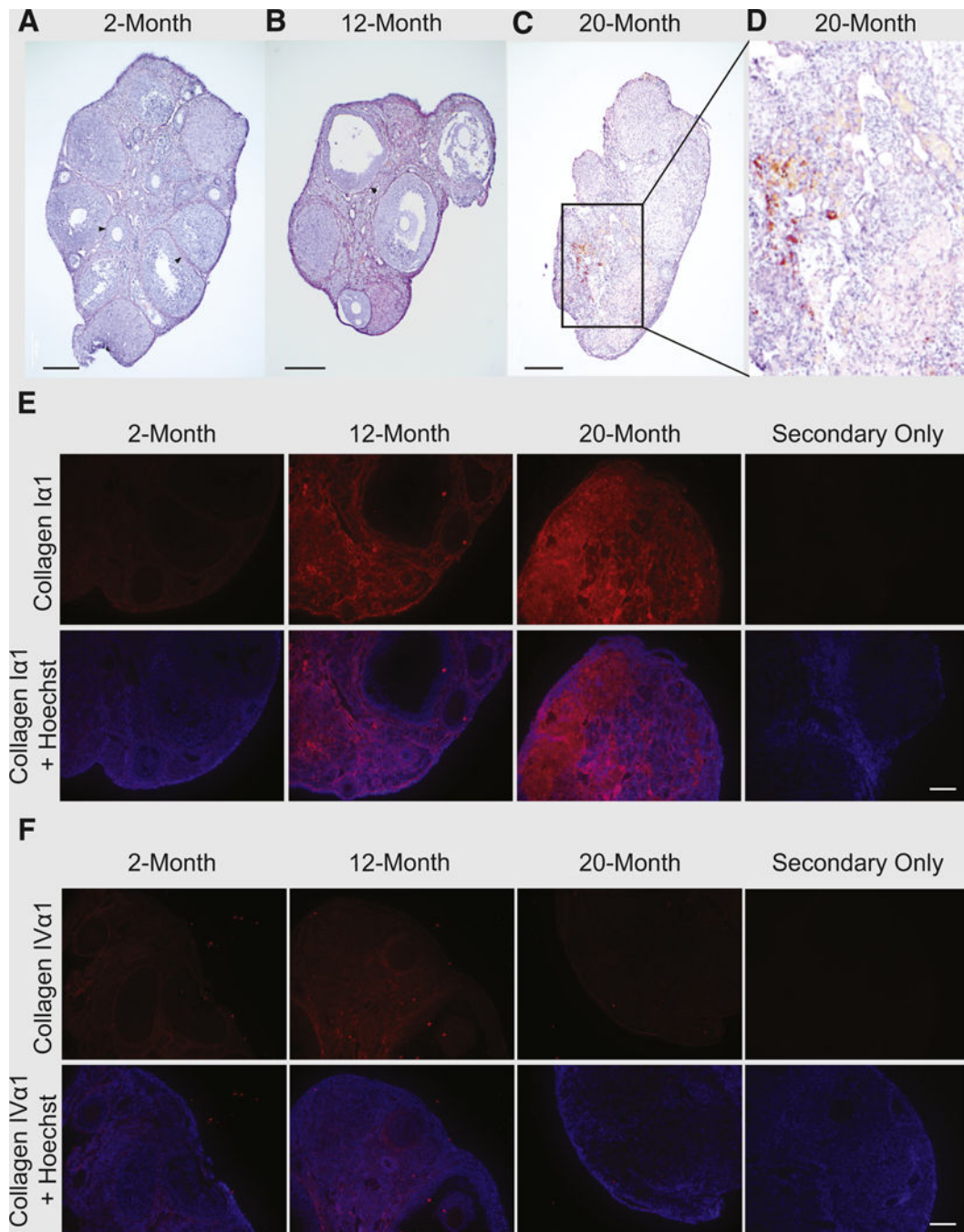
1. Zuckerman S The number of oocytes in the mature ovary. *Recent Prog Horm Res* 1951;6:63–109.
2. Franchi LL, Mandel A, Zuckerman S. The development of the ovary and the process of oogenesis. In: Zuckerman S, editor. *The ovary* New York: Academic Press; 1962:1–88.
3. Gosden RG, Lain SC, Felicio LS, Nelson JF, Finch CE. Imminent oocyte exhaustion and reduced follicular recruitment mark the transition to acyclicity in aging C57BL/6J mice. *Biol Reprod* 1983;28:255–60. [PubMed: 6838945]
4. Richardson SJ, Senikas V, Nelson JF. Follicular depletion during the menopausal transition: evidence for accelerated loss and ultimate exhaustion. *J Clin Endocrinol Metab* 1987;65:1231–7. [PubMed: 3119654]
5. Johnson J, Canning J, Kaneko T, Pru JK, Tilly JL. Germline stem cells and follicular renewal in the postnatal mammalian ovary. *Nature* 2004;428:145–50. [PubMed: 15014492]
6. Albertini DF. Micromanagement of the ovarian follicle reserve—do stem cells play into the ledger? *Reproduction* 2004;127:513–4. [PubMed: 15129006]
7. Byskov AG, Faddy MJ, Lemmen JG, Andersen CY. Eggs forever? *Differentiation* 2005;73:438–46. [PubMed: 16351687]
8. Niikura Y, Niikura T, Tilly JL. Aged mouse ovaries possess rare premeiotic germ cells that can generate oocytes following transplantation into a young host environment. *Aging* 2009;1:971–8. [PubMed: 20157580]
9. Zou K, Yuan Z, Yang Z, Luo H, Sun K, Zhou L, et al. Production of offspring from a germline stem cell line derived from neonatal ovaries. *Nat Cell Biol* 2009;11:631–6. [PubMed: 19363485]
10. Pacchiarotti J, Maki C, Ramos T, Marh J, Howerton K, Wong J, et al. Differentiation potential of germ line stem cells derived from the postnatal mouse ovary. *Differentiation* 2010;79:159–70. [PubMed: 20138422]
11. Wang N, Tilly JL. Epigenetic status determines germ cell meiotic commitment in embryonic and postnatal mammalian gonads. *Cell Cycle* 2010; 9:339–49. [PubMed: 20009537]

12. Zhang Y, Yang Z, Yang Y, Wang S, Shi L, Xie W, et al. Production of transgenic mice by random recombination of targeted genes in female germline stem cells. *J Mol Cell Biol* 2011;3:132–41. [PubMed: 21149239]
13. Zou K, Hou L, Sun K, Xie W, Wu J. Improved efficiency of female germline stem cell purification using Fragilis-based magnetic bead sorting. *Stem Cells Dev* 2011;20:2197–204. [PubMed: 21615296]
14. White YAR, Woods DC, Takai Y, Ishihara O, Seki H, Tilly JL. Oocyte formation by mitotically active germ cells purified from ovaries of reproductive-age women. *Nat Med* 2012;18:413–21. [PubMed: 22366948]
15. Imudia AN, Wang N, Tanaka Y, White YA, Woods DC, Tilly JL. Comparative gene expression profiling of adult mouse ovary-derived oogonial stem cells supports a distinct cellular identity. *Fertil Steril* 2013;100:1451–8. [PubMed: 23876535]
16. Park ES, Woods DC, Tilly JL. Bone morphogenetic protein 4 promotes mammalian oogonial stem cell differentiation via Smad1/5/8 signaling. *Fertil Steril* 2013;100:1468–75. [PubMed: 23993924]
17. Woods DC, Tilly JL. Isolation, characterization and propagation of mitotically active germ cells from adult mouse and human ovaries. *Nat Protoc* 2013;8: 966–88. [PubMed: 23598447]
18. Wang H, Jiang M, Bi H, Chen X, He L, Li X, et al. Conversion of female germline stem cells from neonatal and prepubertal mice into pluripotent stem cells. *J Mol Cell Biol* 2014;6:166–71.
19. Xie W, Wang H, Wu J. Similar morphological and molecular signatures shared by female and male germline stem cells. *Sci Rep* 2014;4:5580. [PubMed: 24993338]
20. Khosravi-Farsani S, Amidi F, Roudkenar MH, Sobhani A. Isolation and enrichment of mouse female germ line stem cells. *Cell J* 2015;16:406–15. [PubMed: 25685731]
21. Park ES, Tilly JL. Use of DEAD-box polypeptide 4 (Ddx4) gene promoter-driven fluorescent reporter mice to identify mitotically active germ cells in postnatal mouse ovaries. *Mol Hum Reprod* 2015;21:58–65. [PubMed: 25147160]
22. Xiong J, Lu Z, Wu M, Zhang J, Cheng J, Luo A, et al. Intraovarian transplantation of female germline stem cells rescues ovarian function in chemo- therapy injured ovaries. *PLoS One* 2015;10:e0139824. [PubMed: 26431320]
23. Guo K, Li CH, Wang XY, He DJ, Zheng P. Germ stem cells are active in postnatal mouse ovary under physiological conditions. *Mol Hum Reprod* 2016; 22:316–28. [PubMed: 26916381]
24. Lu Z, Wu M, Zhang J, Xiong J, Cheng J, Shen W, et al. Improvement in isolation and identification of mouse oogonial stem cells. *Stem Cells Int* 2016; 2016:2749461. [PubMed: 26635882]
25. Zhang C, Wu J. Production of offspring from a germline stem cell line derived from prepubertal ovaries of germline reporter mice. *Mol Hum Reprod* 2016; 22:457–64. [PubMed: 27141102]
26. Zhang XL, Wu J, Wang J, Shen T, Li H, Lu J, et al. Integrative epigenomic analysis reveals unique epigenetic signatures involved in unipotency of mouse female germline stem cells. *Genome Biol* 2016;17:162. [PubMed: 27465593]
27. Wang N, Satirapod C, Ohguchi Y, Park ES, Woods DC, Tilly JL. Genetic studies in mice directly link oocytes produced during adulthood to ovarian function and natural fertility. *Sci Rep* 2017;7:10011. [PubMed: 28855574]
28. Wu C, Xu B, Li X, Ma W, Zhang P, Wu J. Tracing and characterizing the development of transplanted female germline stem cells in vivo. *Mol Ther* 2017; 25:1408–19. [PubMed: 28528817]
29. Ye H, Zheng T, Hu C, Pan Z, Huang J, Li J, et al. The Hippo signaling pathway regulates ovarian function via the proliferation of ovarian germline stem cells. *Cell Physiol Biochem* 2017;41:1051–62. [PubMed: 28245464]
30. Wang J, Gong X, Tian GG, Hou C, Zhu X, Pei X, et al. Long noncoding RNA growth arrest-specific 5 promotes proliferation and survival of female germ- line stem cells in vitro. *Gene* 2018;653:14–21. [PubMed: 29428796]
31. Wu M, Xiong J, Ma L, Lu Z, Qin X, Luo A, et al. Enrichment of female germline stem cells from mouse ovaries using the differential adhesion method. *Cell Physiol Biochem* 2018;46:2114–26. [PubMed: 29723864]

32. Yang H, Yao X, Tang F, Wei Y, Hua J, Peng S. Characterization of female germline stem cells from adult mouse ovaries and the role of rapamycin on them. *Cytotechnology* 2018;70:843–54. [PubMed: 29372468]
33. Zhu X, Tian GG, Yu B, Yang Y, Wu J. Effects of bisphenol A on ovarian follicular development and female germline stem cells. *Arch Toxicol* 2018;92: 1581–91. [PubMed: 29380011]
34. Gu Y, Wu J, Yang W, Xia C, Shi X, Li H, et al. STAT3 is required for proliferation and exerts a cell type-specific binding preference in mouse female germline stem cells. *Mol Omics* 2018;14:95–102. [PubMed: 29659651]
35. Zhang HY, Yang Y, Xia Q, Song HF, Wei R, Wang JJ, et al. Cadherin 22 participates in the self-renewal of mouse female germline stem cells via interaction with JAK2 and b-catenin. *Cell Mol Life Sci* 2018;75:1241–53. [PubMed: 29063123]
36. Zhou L, Wang L, Kang JX, Xie W, Li X, Wu C, et al. Production of fat-1 transgenic rats using a post-natal female germline stem cell line. *Mol Hum Reprod* 2014;20:271–81. [PubMed: 24258451]
37. Tsai T-S, Johnson J, White Y, St John JC. The molecular characterization of porcine egg precursor cells. *Oncotarget* 2017;8:63484–505. [PubMed: 28969006]
38. Hou L, Wang J, Wang H, Liu G, Xu B, Mei X, et al. Characteristics of female germline stem cells from porcine ovaries at sexual maturity. *Cell Transplant* 2018;27:1195–202. [PubMed: 29991280]
39. de Souza GB, Costa J, da Cunha EV, Passos J, Ribeiro RP, Saraiva M, et al. Bovine ovarian stem cells differentiate into germ cells and oocyte-like structures after culture in vitro. *Reprod Domest Anim* 2017;52:243–50. [PubMed: 27925309]
40. Woods DC, Tilly JL. Reply to adult human and mouse ovaries lack DDX4-expressing functional oogonial stem cells. *Nat Med* 2015;21:1118–21. [PubMed: 26444632]
41. Ding X, Liu G, Xu B, Wu C, Hui N, Ni X, et al. Human GV oocytes generated by mitotically active germ cells obtained from follicular aspirates. *Sci Rep* 2016;6:28218. [PubMed: 27357640]
42. Clarkson YL, McLaughlin M, Waterfall M, Dunlop CE, Skehel PA, Anderson RA, et al. Initial characterisation of adult human ovarian cell populations isolated by DDX4 expression and aldehyde dehydrogenase activity. *Sci Rep* 2018;8:6953. [PubMed: 29725036]
43. Silvestris E, Cafforio P, d’Oronzo S, Felici C, Silvestris F, Loverro G. In vitro differentiation of human oocyte-like cells from oogonial stem cells: single-cell isolation and molecular characterization. *Hum Reprod* 2018;33:464–73. [PubMed: 29304224]
44. Bothun A, Gao Y, Takai Y, Ishihara O, Seki H, Karger B, et al. Quantitative proteomic profiling of the human ovary from early to mid-gestation reveals protein expression dynamics of oogenesis and folliculogenesis. *Stem Cells Dev* 2018;27:723–35. [PubMed: 29631484]
45. Tilly JL, Telfer EE. Purification of germline stem cells from adult mammalian ovaries: a step closer toward control of the female biological clock? *Mol Hum Reprod* 2009;15:393–8. [PubMed: 19509111]
46. Woods DC, Tilly JL. The next (re)generation of human ovarian biology and female fertility: is current science tomorrow’s practice? *Fertil Steril* 2012; 98:3–10. [PubMed: 22682028]
47. Woods DC, Telfer EE, Tilly JL. Oocyte family trees: old branches or new stems? *PLoS Genet* 2012;8:e1002848. [PubMed: 22844256]
48. Woods DC, Tilly JL. Germline stem cells in adult mammalian ovaries. In: Sanders S, editor. *Ten critical topics in reproductive medicine* Washington, DC: Science/AAAS; 2013:10–2.
49. Woods DC, Tilly JL. An evolutionary perspective on adult female germline stem cell function from flies to humans. *Semin Reprod Med* 2013;31:24–32. [PubMed: 23329633]
50. Grieve KM, McLaughlin M, Dunlop CE, Telfer EE, Anderson RA. The controversial existence and functional potential of oogonial stem cells. *Maturitas* 2015;82:278–81. [PubMed: 26278874]
51. Fakh MH, El Shmoury M, Szeptycki J, dela Cruz DB, Lux C, Verjee S, et al. The AUGMENT treatment: physician reported outcomes of the initial global patient experience. *JFIV Reprod Med Genet* 2015;3:154.
52. Oktay K, Baltaci V, Sonmezer M, Turan V, Unsal E, Baltaci A, et al. Oogonial precursor cell-derived autologous mitochondria injection to improve outcomes in women with multiple IVF failures due to low oocyte quality: a clinical translation. *Reprod Sci* 2015;22:1612–7. [PubMed: 26567266]

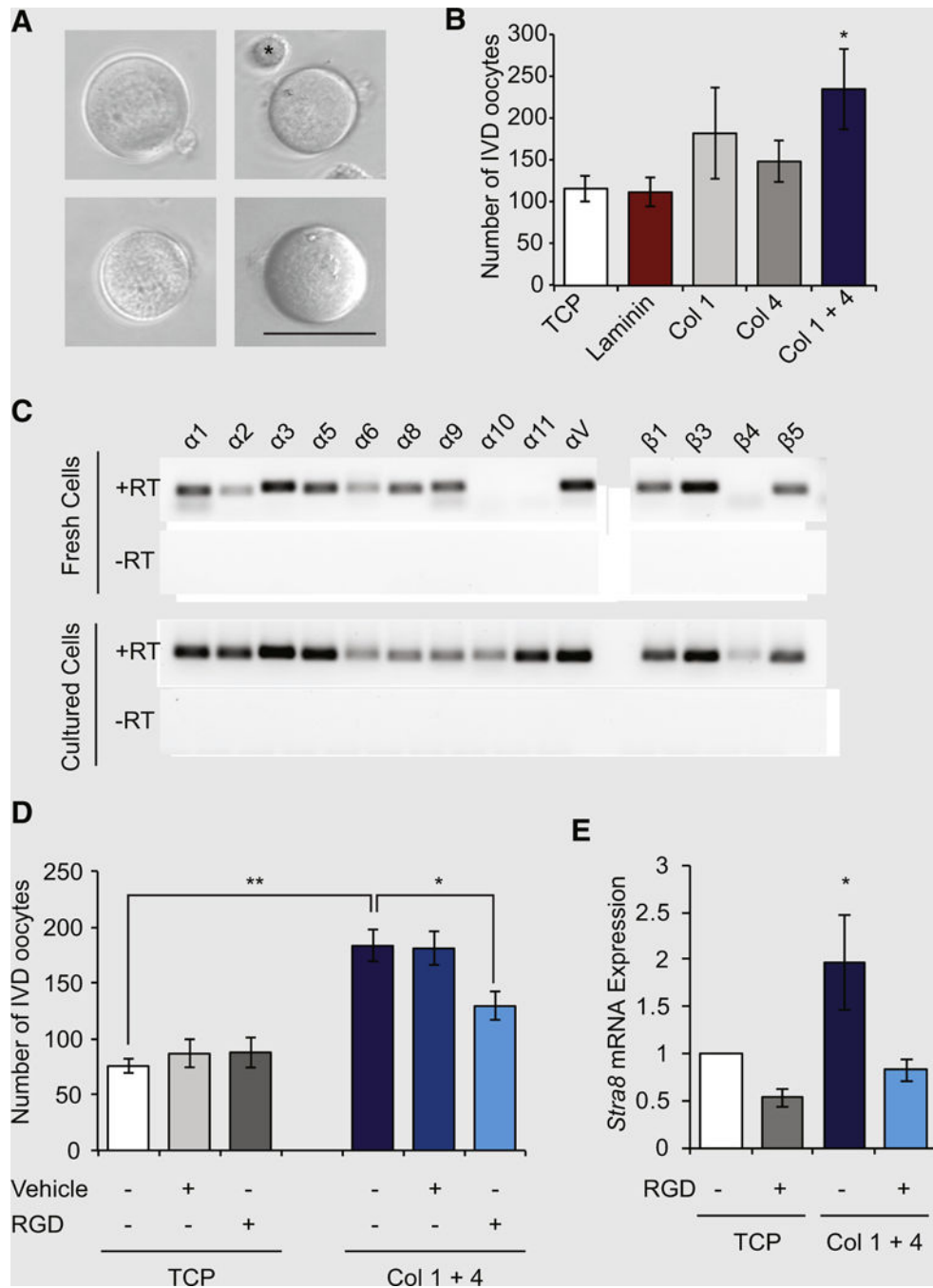
53. Woods DC, Tilly JL. Autologous germline mitochondrial energy transfer (AUGMENT) in human assisted reproduction. *Semin Reprod Med* 2015; 33:410–21. [PubMed: 26574741]
54. Braam SR, Zeinstra L, Litjens S, Ward-van Oostwaard D, van den Brink S, van Laake L, et al. Recombinant vitronectin is a functionally defined substrate that supports human embryonic stem cell self-renewal via α V β 5 integrin. *Stem Cells* 2008;26:2257–65. [PubMed: 18599809]
55. Guilak F, Cohen DM, Estes BT, Gimble JM, Liedtke W, Chen CS. Control of stem cell fate by physical interactions with the extracellular ma. *Cell Stem Cell* 2009;5:17–26. [PubMed: 19570510]
56. Rodin S, Antonsson L, Hovatta O, Tryggvason K. Monolayer culturing and cloning of human pluripotent stem cells on laminin-521-based matrices under xeno-free and chemically defined conditions. *Nat Protoc* 2014;9:2354–68. [PubMed: 25211513]
57. Laperle A, Hsiao C, Lampe M, Mortier J, Saha K, Palecek SP, et al. α -5-Laminin synthesized by human pluripotent stem cells promotes self-renewal. *Stem Cell Rep* 2015;5:195–206.
58. Engler AJ, Sen S, Sweeney HL, Discher DE. Matrix elasticity directs stem cell lineage specification. *Cell* 2006;126:677–89. [PubMed: 16923388]
59. Rossi DJ, Bryder D, Zahn JM, Ahlenius H, Sonu R, Wagers AJ, et al. Cell intrinsic alterations underlie hematopoietic stem cell aging. *Proc Natl Acad Sci USA* 2005;102:9194–9. [PubMed: 15967997]
60. Ryu BY, Orwig KE, Oatley JM, Avarbock MR, Brinster RL. Effects of aging and niche microenvironment on spermatogonial stem cell self-renewal. *Stem Cells* 2006;24:1505–11. [PubMed: 16456131]
61. Brack A, Conboy M, Roy S, Lee M, Kuo CJ, Keller C, et al. Increased Wnt signaling during aging alters muscle stem cell fate. *Science* 2007;317: 807–10. [PubMed: 17690295]
62. Giangreco A, Qin M, Pintar JE, Watt FM. Epidermal stem cells are retained in vivo throughout skin aging. *Aging Cell* 2008;7:250–9. [PubMed: 18221414]
63. Wagner W, Horn P, Bork S, Ho AD. Aging of hematopoietic stem cells is regulated by the stem cell niche. *Exp Gerontol* 2008;43:974–80. [PubMed: 18504082]
64. Jung Y, Brack AS. Cellular mechanisms of somatic stem cell aging. *Curr Top Dev Biol* 2014;107:405–38. [PubMed: 24439814]
65. Irving-Rodgers HF, Rodgers RJ. Extracellular matrix in ovarian follicular development and disease. *Cell Tissue Res* 2005;322:89–98. [PubMed: 16158327]
66. Irving-Rodgers HF, Rodgers RJ. Extracellular matrix of the developing ovarian follicle. *Semin Reprod Med* 2006;24:195–203. [PubMed: 16944417]
67. Berkholtz CB, Lai BE, Woodruff TK, Shea LD. Distribution of extracellular matrix proteins type I collagen, type IV collagen, fibronectin, and laminin in mouse folliculogenesis. *Histochem Cell Biol* 2006;126:583–92. [PubMed: 16758163]
68. Oktay K, Karlikaya G, Akman O, Ojakian GK, Oktay M. Interaction of extra-cellular matrix and activin-A in the initiation of follicle growth in the mouse ovary. *Biol Reprod* 2000;63:457–61 [PubMed: 10906050]
69. Laszczynska M, Brodowska A, Starczewski A, Masiuk M, Brodowski J. Human postmenopausal ovary—hormonally inactive fibrous connective tissue or more? *Histol Histopathol* 2008;23:219–26. [PubMed: 17999378]
70. Irving-Rodgers HF, Hummitzsch K, Murdiyarslo LS, Bonner WM, Sado Y, Ninomiya Y, et al. Dynamics of extracellular matrix in ovarian follicles and corpora lutea of mice. *Cell Tissue Res* 2010;339:613–24. [PubMed: 20033213]
71. Lind AK, Weijdegård B, Dahm-Kähler P, Mölne J, Sundfeldt K, Brännström M. Collagens in the human ovary and their changes in the perifollicular stroma during ovulation. *Acta Obstet Gynecol Scand* 2006;85:1476–84. [PubMed: 17260225]
72. Laronda MM, Rutz AL, Xiao S, Whelan KA, Duncan FE, Roth EW, et al. A bioprosthetic ovary created using 3D printed microporous scaffolds restores ovarian function in sterilized mice. *Nat Commun* 2017;8:15261. [PubMed: 28509899]
73. Reddy GK, Enwemeka CS. A simplified method for the analysis of hydroxyproline in biological tissues. *Clin Biochem* 1996;29:225–9. [PubMed: 8740508]

74. Naba A, Clauser KR, Hoersch S, Liu H, Carr SA, Hynes RO. The matrisome: in silico definition and in vivo characterization by proteomics of normal and tumor extracellular matrices. *Mol Cell Proteomics* 2011;11:M111, 014647.
75. Hynes RO, Naba A. Overview of the matrisome—an inventory of extracellular matrix constituents and functions. *Cold Spring Harb Perspect Biol* 2012;4:a004903. [PubMed: 21937732]
76. Massasa E, Costa XS, Taylor HS. Failure of the stem cell niche rather than loss of oocyte stem cells in the aging ovary. *Aging* 2010;2:1–2. [PubMed: 20228937]
77. Martin JJ, Woods DC, Tilly JL. Implications and current limitations of oogenesis from female germline or oogonial stem cells in adult mammalian ovaries. *Cells* 2019;8:93 10.3390/cells8020093.
78. Woodruff TK, Shea LD. The role of the extracellular matrix in ovarian follicle development. *Reprod Sci* 2007;14:6–10.
79. Shea LD, Woodruff TK, Shikanov A. Bioengineering the ovarian follicle microenvironment. *Annu Rev Biomed Eng* 2014;16:29–52. [PubMed: 24849592]
80. Kurilo LF. Oogenesis in antenatal development in man. *Hum Genet* 1981; 57:86–92. [PubMed: 7262874]
81. Konishi I, Fujii S, Okamura H, Parmley T, Mori T. Development of interstitial cells and ovigerous cords in the human fetal ovary: an ultrastructural study. *J Anat* 1986;148:121–35. [PubMed: 3693081]
82. Kalamajski S, Oldberg A. The role of small leucine-rich proteoglycans in collagen fibrillogenesis. *Matrix Biol* 2010;9:248–53.
83. Ouni E, Vertommen D, Chiti MC, Dolmans MM, Amori CA. A draft map of the human ovarian proteome for tissue engineering and clinical applications. *Mol Cell Proteomics* 2018 Available at: 10.1074/mcp.RA117.000469.
84. Sawada Y, Sato T, Saito C, Ozawa F, Ozaki Y, Sugiura-Ogasawara M. Clinical utility of decorin in follicular fluid as a biomarker of oocyte potential. *Reprod Biol* 2017;18:33–9. [PubMed: 29229446]
85. Tran H, VanDusen WJ, Argraves WS. The self-association and fibronectin-binding sites of fibulin-1 map to calcium-binding epidermal growth factor-like domains. *J Biol Chem* 1997;272:22600–6. [PubMed: 9278415]
86. Bouma GJ, Hudson QJ, Washburn LL, Eicher EM. New candidate genes identified for controlling mouse gonadal sex determination and the early stages of granulosa and Sertoli cell differentiation. *Biol Reprod* 2010;82: 380–9. [PubMed: 19864314]

**FIGURE 1.**

(A–D) Van Gieson staining (*blue*: nuclei; *red*: collagen; *yellow*: cytoplasm), showing development of tissue fibrosis and disorganization of collagen with advancing age. (A) Ovaries of 2-month-old mice exhibit fibrillar organization of collagenous basement membranes surrounding follicles (examples indicated by *arrowheads*). (B) Late-reproductive-age ovarian tissue shows decreasing organization of collagen disseminating throughout the tissue, while still bounding follicles (*arrowhead*). (C, D) Postreproductive (aged) ovarian tissue shows large areas of tissue fibrosis. (E, F) Antibody labeling of

extracellular matrix (ECM) component proteins (**E**) type I collagen ($I\alpha 1$ subunit) and (**F**) type IV collagen ($IV\alpha 1$ subunit) shows subtype-specific changes in ECM with age. Representative images of ovaries from three animals processed for each age group with primary antibody. Scale bars = 200 μm (**A–D**), 50 μm (**E, F**).

**FIGURE 2.**

(A) Representative images of in vitro derived (IVD) oocytes formed by mouse oogonial stem cells (mOSCs) in culture. Scale bar 50- μ m. Asterisk (upper right panel) highlights an OSC shown for size comparison to an adjacent IVD oocyte. (B) Number of IVD oocytes formed in cultures of mOSCs seeded onto tissue culture plastic (TCP), laminin, type I collagen (Col 1), type IV collagen (Col 4) or a mixture of the two collagens (Col 1 + 4; 10 μ g/ cm^2 of a 1:1 mixture) for 72 hours (mean \pm SEM; n = 5; * P < .05 vs. TCP). (C) Representative expression analysis of known matrix-binding integrin subunits in freshly

isolated (fresh) or passage 35 (cultured) mOSCs (+RT and –RT = addition and exclusion of reverse transcriptase for the reverse-transcription polymerase chain reaction analysis to rule out the possibility of signal resulting from amplification of genomic DNA). **(D)** Treatment of mOSCs with the integrin-neutralizing peptide Arg-Gly-Asp (RGD; 500 $\mu\text{mol/L}$) inhibits the increase in mOSC differentiation induced by a mixture of type I and type IV collagens (mean T SEM; $n = 3$; * $P < .05$; ** $P < .01$). **(E)** Addition of RGD peptide inhibits the ability of the collagen mixture to increase expression of the meiotic commitment gene *Stra8* in cultured mOSCs ($n = 5$; * $P < .05$).

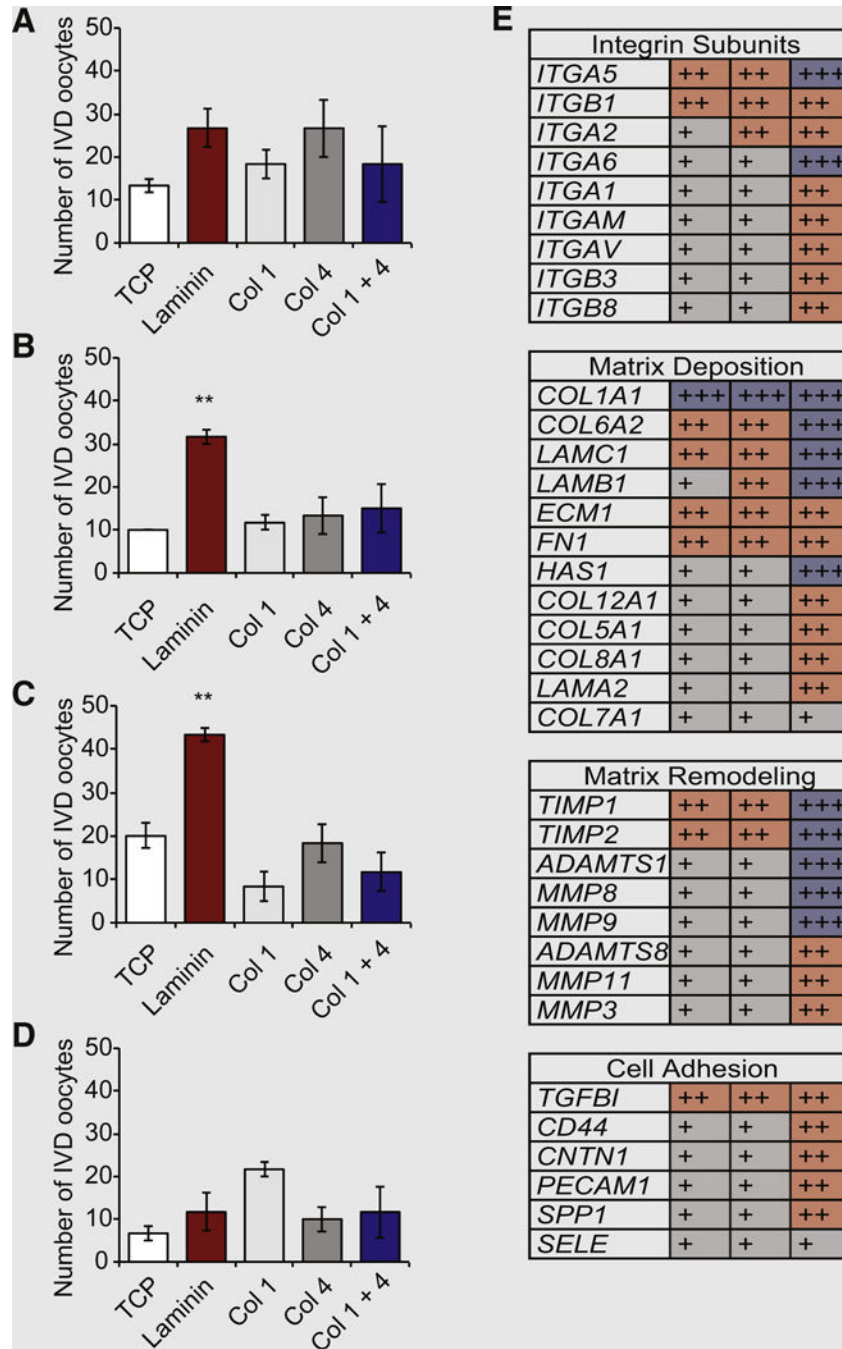


FIGURE 3. (A–D) Numbers of IVD oocytes formed by human oogonal stem cells (hOSCs) cultured for (A) 24, (B) 48, (C) 72, or (D) 96 hours on TCP or TCP coated with laminin, type I collagen (Col 1), type IV collagen (Col 4), or a mixture of the two collagens (Col 1 + 4; 10 $\mu\text{g}/\text{cm}^2$ of a 1:1 mixture; mean SEM; n = 3; ** $P < .01$ vs. TCP). Abbreviations as in Figure 2. (E) Microarray expression analysis of multiple components of the integrin signaling network in three independent hOSC lines (each hOSC line, established from ovarian tissue of different subjects, is represented in a single column). The intensity of expression was normalized

against *GAPDH* levels as low (+, *gray shaded boxes*), moderate (++, *red shaded boxes*) and high (+++, *blue shaded boxes*).

Author Manuscript

Author Manuscript

Author Manuscript

Author Manuscript

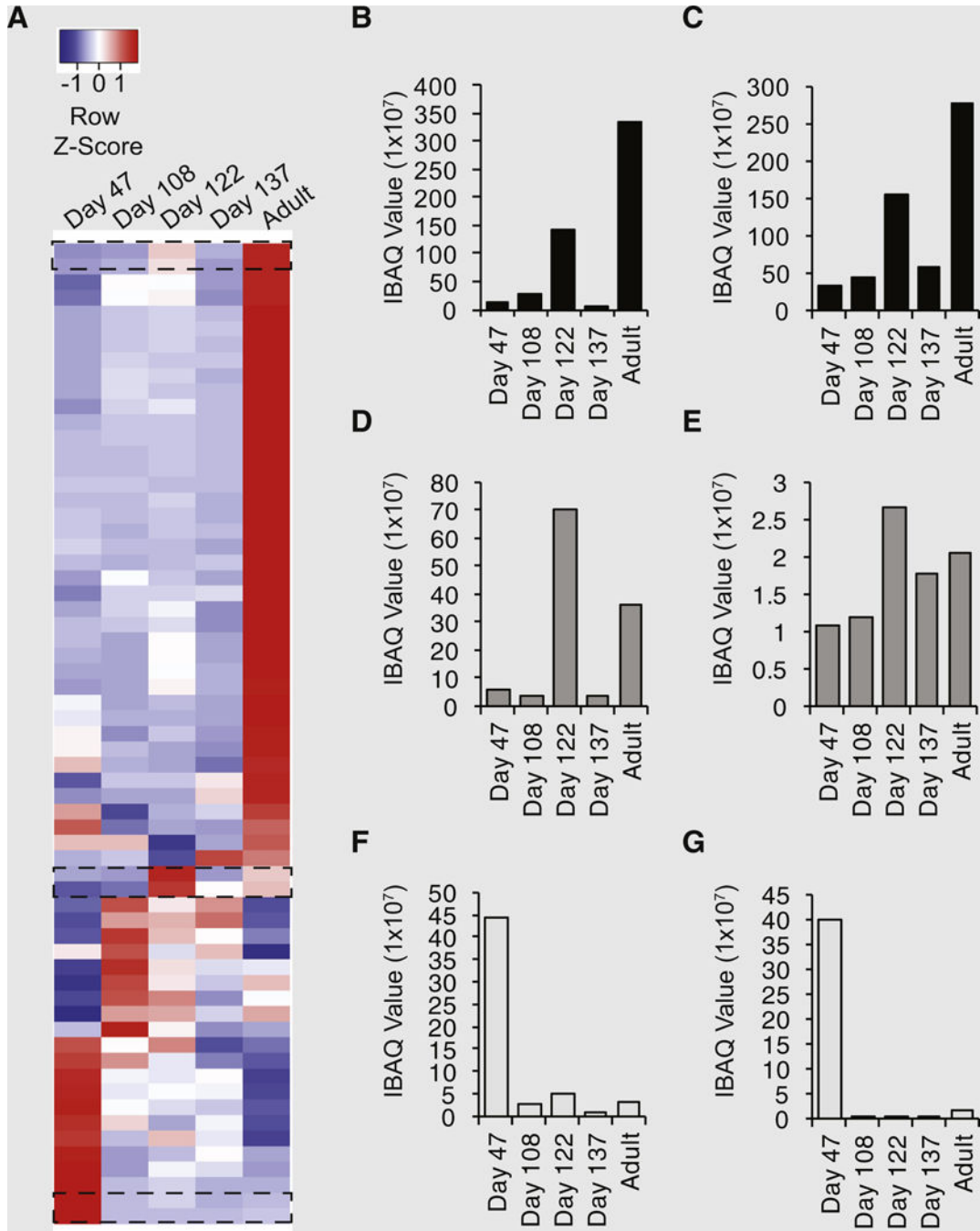


FIGURE 4. (A) In silico analysis of a public proteomic database of fetal human ovarian tissue from gestational days 47, 108, 122, and 137, as well as adult human ovarian cortical tissue, for components of the human matrisome. Average linkage hierarchic clustering based on sample intensity-based absolute quantification values displayed developmental stage-specific changes in the human ovarian matrisome, with *red* indicating high expression and *blue* indicating low expression relative to each identified protein. *Dashed boxes* indicate proteins of interest for further analysis in panels B–G. (B–G) The small leucine-rich proteoglycans

(B) decorin and **(C)** lumican exhibited the highest relative expression in adult ovarian cortex versus fetal ovaries, whereas **(D)** osteoglycin and **(E)** laminin gamma chain were most abundant at gestational day 122; **(F)** fibulin-1 and **(G)** protein C inhibitor had the highest relative expression levels at the earliest developmental stage (day 47).